Aqueous Solution Speciation of Fe(III) Complexes with Dihydroxamate Siderophores Alcaligin and Rhodotorulic Acid and Synthetic Analogues Using Electrospray Ionization Mass Spectrometry

Ivan Spasojević,[†] Hakim Boukhalfa,[†] Robert D. Stevens,[‡] and Alvin L. Crumbliss*,[†]

Department of Chemistry, Duke University, Box 90346, Durham, North Carolina 27708, and Mass Spectrometry Facility, Duke University Medical Center, Durham, North Carolina 27710

Received December 2, 1999

Aqueous solutions of Fe^{3+} complexes of cyclic (alcaligin) and linear (rhodotorulic acid) dihydroxamate siderophores and synthetic linear eight-carbon-chain and two-carbon-chain dihydroxamic acids ($[CH_3N(OH)C{=}O)]_2(CH_2)_n$; H_2L^n; $n = 2$ and 8) were investigated by electrospray ionization mass spectrometry (ESI-MS). Information was obtained relevant to the structure and the speciation of various Fe(III)−dihydroxamate complexes present in aqueous solution by (1) comparing different ionization techniques (ESI and FAB), (2) altering the experimental parameters (Fe^{3+}/ligand ratio, pH, cone voltage), (3) using high-stability hexacoordinated Fe(III) siderophore complex mixtures (ferrioxamine B/ferrioxamine E) as a calibrant to quantify intrinsically neutral (H^+ clustered or protonated) and intrinsically charged complexes, and (4) using mixed-metal complexes containing Fe^{3+}, Ga^{3+}, and Al^{3+}. These results illustrate that for all dihydroxamic acid ligands investigated multiple tris- and bis-chelated mono- and di-Fe(III) species are present in relative concentrations that depend on the pH and Fe/L ratio.

Introduction[1]

Siderophores are microbially synthesized molecules that solubilize environmental Fe(III) by chelation. These siderophores are of varied structure, with differing numbers of hydroxamate, catecholate, and/or α-hydroxycarboxylate Fe(III) binding groups in different architectures.[2−6] Knowledge of the structure, stability, and reactivity of these Fe(III) complexes with siderophore ligands of differing denticity is of importance in developing our understanding of siderophore-mediated Fe bioavailability, as well as understanding of the coordination chemistry and self-assembly processes associated with mono- and multicentered Fe(III) complexes. The tetradentate dihydroxamic acids (Figure 1) are unable to satisfy the preferred octahedral coordination geometry of Fe(III) by forming simple 1:1 complexes, as in the case of the hexadentate trihydroxamate ligands (e.g., desferrioxamine B and desferrioxamine E). Instead, a dihydroxamate siderophore must form bimetallic complexes with a stoichiometry such as Fe_2L_3 (LH_2 represents the dihydroxamate ligand),[1] which is the minimal stoichiometry needed for the complete coordination of the metal ion. Rhodotorulic acid, a linear natural dihydroxamate siderophore (Figure 1), was reported to form a triply bridged complex with Fe based on CD spectra and potentiometric titrations.[7,8] An X-ray crystal structure has been obtained for an analogous triply bridged dihydroxypyridinone complex of Fe(III).[9] Recent studies of a *cyclic* natural dihydroxamate siderophore, alcaligin (Figure 1),

* To whom correspondence should be addressed. E-mail: alc@chem.duke.edu. Fax: 919-660-1605.

[†] Duke University.

[‡] Duke University Medical Center.

(1) Nomenclature and abbreviations: "mono" represents a dicoordinated metal complex with one bound hydroxamate group. "bis" represents a tetracoordinated metal complex with two bound hydroxamate groups, and "tris" represents a hexacoordinated metal complex with three bound hydroxamate groups, not all of which are necessarily from the same ligand molecule. H_2L^n represents the linear synthetic dihydroxamic acid, $[CH_3N(OH)C{=}O)]_2(CH_2)_n$, where H_2L^2 corresponds to a two-carbon chain ($n = 2$) and H_2L^8 corresponds to an eight-carbon chain ($n = 8$) linking the hydroxamate moieties (Figure 1). $(HL^n)^-$ and $(L^n)^{2-}$ represent the singly and doubly deprotonated dihydroxamic acid ligand, respectively. H_2L^{RA} and H_2L^{AG} correspond to the dihydroxamic acid siderophores rhodotorulic acid and alcaligin, respectively (Figure 1). Structural representations are as follows. **$Fe(L^nH)_3$** is a tris-chelated complex with three bound hydroxamate groups from each of three monodeprotonated dihydroxamate ligands. (L^n) units placed between two Fe atoms represent bridging ligands bound to both Fe atoms. For example, **$(HL^n)Fe(L^n)_2Fe(L^nH)$** represents two tris-chelated Fe(III) centers held together by two bridging dihydroxamate ligands. Coordinated H_2O is omitted for clarity so that **$Fe(L^8)^+$** represents Fe(III) tetracoordinated by a single dihydroxamate ligand with two coordinated H_2O molecules not shown. For ease of reading, structural formulas are shown in bold type, and when a neutral species is observed as a result of protonation in the ESI process, the cluster H^+ is not shown in bold. For example, **$(L^n)Fe(L^nH)(H^+)$** represents the uncharged tris complex **$(L^n)Fe(L^nH)$**, which has been protonated in the ESI experiment to give a +1 charge on the species, while **$Fe(L^nH)_2^+$** represents the bis complex which carries a +1 charge. Percentages in the tables and text represent the ESI-MS peak intensity relative to the highest intensity Fe-containing species.

(2) Albrecht-Gary, A.-M.; Crumbliss, A. L. In *Iron Transport and Storage in Microorganisms, Plants and Animals*; Sigel, A., Sigel, H., Eds.; Metal Ions in Biological Systems 35; M. Dekker, Inc.: New York, 1998; p 239.

(3) Raymond, K. N.; Telford, J. R. In *Bioinorganic Chemistry: An Inoganic Perspective of Life*; Kessissoglou, D. P., Ed.; NATO ASI Series C: Mathematical and Physical Science 459; Kluwer Academic Publishers: Dordrecht, The Netherlands, 1995; p 25.

(4) Crumbliss, A. L. In *Handbook of Microbial Iron Chelates*; Winkelmann, G., Ed.; CRC Press: Boca Raton, FL, 1991; p 177.

(5) Telford, J. R.; Raymond, K. N. In *Molecular Recognition: Receptors for Cationic Guests*; Lehn, J.-M., Gokel. G. W., Eds.; Comprehensive Supramolecular Chemistry 1; Pergamon Press: London, 1996; p 245.

(6) Drechsel, H.; Winkelmann, G. In *Transition Metals in Microbial Metabolism*; Winkelmann, G., Carrano, C. J., Eds.; Harwood Academic Publishers: Amsterdam, 1997; p 1.

(7) Carrano, C. J.; Raymond, K. N. *J. Am. Chem. Soc.* **1978**, *100*, 5371.

(8) Carrano, C. J.; Cooper, S. R.; Raymond, K. N. *J. Am. Chem. Soc.* **1979**, *101*, 599.

(9) Scarrow, R. C.; White, D. L.; Raymond, K. N. *J. Am. Chem. Soc.* **1985**, *107*, 6540.

10.1021/ic991390x CCC: $20.00 © 2001 American Chemical Society
Published on Web 12/07/2000

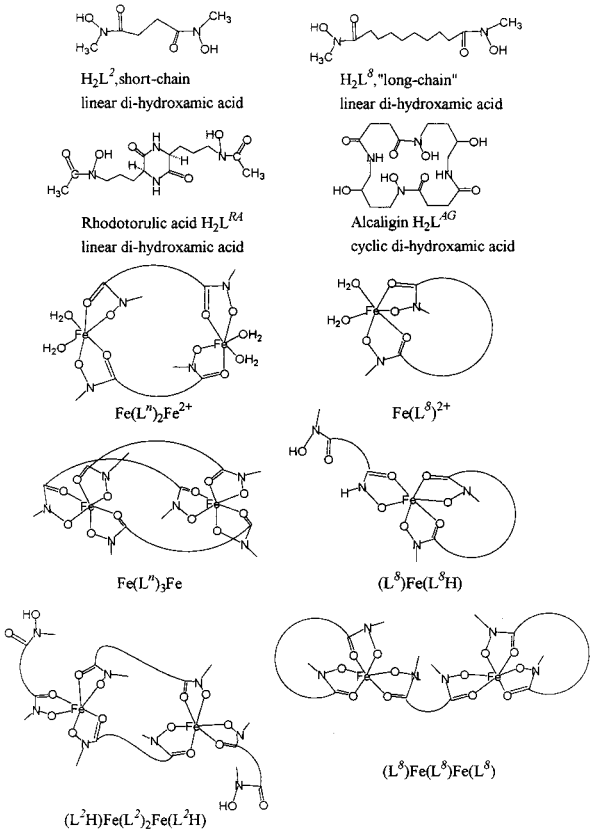

Figure 1. Dihydroxamic acid ligands investigated.

include the first crystallographically characterized structure of an Fe_2L_3 complex containing a natural siderophore.[10,11] This study revealed a preorganized ligand structure for the formation of an $Fe(L^{AG})^+$ complex and a *singly* bridged structure for the fully coordinated 2:3 Fe/L complex $(L^{AG})Fe(L^{AG})Fe(L^{AG})$.[1]

Synthetic dihydroxamate ligands of different carbon chain lengths ($[CH_3N(OH)C{=}O)]_2(CH_2)_n$; H_2L^n)[1] have been prepared in our laboratory as mimics for the dihydroxamate siderophores. Their Fe(III) complexes at 1:1 Fe/L ratio have been characterized by electrospray ionization mass spectrometry (ESI-MS) as $Fe(L^n)^+$ and $Fe(L^n)_2Fe^{2+}$, depending on the chain length *n* between the hydroxamate groups,[12,13] and by their pH jump ligand dissociation kinetics analyzed at 1:1[14] and lower[15] Fe/L ratios. The pH jump ligand dissociation kinetics were also investigated for Fe(III) complexes of rhodotorulic acid and alcaligin.[16] The mechanism of tris-complex ligand dissociation shows a high level of complexity, with numerous stable intermediates present in solution and multiple pathways to complete ligand dissociation.

In this study, we present a systematic investigation of the species formed between $Fe^{3+}{}_{aq}$ and the synthetic dihydroxamic acids H_2L^n ($n = 2, 8$), and the natural siderophores rhodotorulic acid and alcaligin (Figure 1) using electrospray ionization mass spectrometry. The purpose of this investigation is to characterize the speciation and structure of the complexes formed at different Fe/L ratios and pH values and to explore the use of mixed-metal complexes containing Al^{3+}, Fe^{3+}, and Ga^{3+} to further characterize the coordination chemistry of the dihydroxamate ligands. This work is also intended to explore the scope and limits of ESI-MS as a "gentle" ionization technique to probe metal−ligand complex equilibria in aqueous solution. The use of ESI-MS to study metal complexes in solution has been recently reviewed.[17,18]

Experimental Section

The dihydroxamic acid ligands (H_2L^2 and H_2L^8)[1] were prepared according to the method described in the literature[19,20] and were recrystallized and characterized as described elsewhere.[14] Rhodotorulic acid (H_2L^{RA}) (Aldrich), alcaligin (H_2L^{AG}) (gift from S. K. Armstrong and T. J. Brickman, University of Minnesota), desferrioxamine B, and desferrioxamine E (gift from I. Fridovich, Duke University) were characterized as described elsewhere.[21]

Solutions for ESI-MS analysis (1 mM unless otherwise stated) were prepared by mixing appropriate amounts of the ligand with the desired equivalent of 0.1 M $M(ClO_4)_3$ ($M = Fe^{3+}$, Ga^{3+}, Al^{3+}) in 0.1 M $HClO_4$. The pH was adjusted to the desired acidity by addition of 0.1 M NH_4OH or 0.1 M $HClO_4$; a semiconductor (FET) pH electrode was used in order to avoid solution contamination from the background electrolyte in conventional reference electrodes. All dihydroxamate−Fe(III) solutions were checked by UV−vis spectroscopy and their spectra compared to known complexes in the literature.[7,8,11,14] At pH 2 the Fe(III)-containing complexes exhibited a strong absorbance band characteristic of a bis-Fe(III)−hydroxamate complex ($\lambda_{max} = 470$ nm), while at neutral pH the Fe(III)-containing complexes prepared under the conditions Fe/L $\leq$ 2:3 showed absorbance spectra characteristic of a tris-Fe(III)−hydroxamate complex ($\lambda_{max} = 425-430$ nm).

ESI-MS measurements were made using a Micromass VG BIO-Q triple quadrupole mass spectrometer equipped with a pneumatically assisted electrospray ion source operating at atmospheric pressure. All experiments were performed in positive ion mode and at 40 V cone voltage unless otherwise stated. The mobile phase was *pure water*, and a sample flow rate of 6 μL/min was provided by a syringe pump. The instrument was operated at unit mass resolution, and the mass scale was calibrated using poly(ethylene glycol). Fast-atom-bombardment (FAB) measurements were made using a JEOL JMS SX 102A mass spectrometer in (+) ion mode and with glycerol as a sample matrix.

Results

General Solution Behavior and Preliminary Considerations. Fe(III) forms mono, bis, and tris complexes with the bidentate hydroxamate moiety (−C(=O)−N(O^-)−), each with a characteristic UV−visible spectrum. The fully coordinated tris-iron(III)−hydroxamate complexes are stable at neutral pH and are characterized by an absorption maximum at ca. 430 nm. Increasing the solution acidity to pH 2 results in a conversion of the tris complex to a bis species with an absorption maximum at ca. 470 nm. Further acidification to pH 1 shifts the absorbance maximum to 500 nm because of monohydroxamate complex formation.[7,8,11] The 3+ oxidation state for Fe is stabilized through hydroxamate coordination, as illustrated by redox potentials for *N*-alkyl hydroxamic acid complexes in the range −500 to −350 mV (vs NHE).[21] Because of the large negative

(10) Hou, Z.; Sunderland, C. J.; Nishio, T.; Raymond, K. N. *J. Am. Chem. Soc.* **1996**, *118*, 5148.
(11) Hou, Z.; Raymond, K. N.; O'Sullivan, B.; Esker, T. W.; Nishio, T. *Inorg. Chem.* **1998**, *37*, 6630.
(12) Caudle, M. T.; Stevens, R. D.; Crumbliss, A. L. *Inorg. Chem.* **1994**, *33*, 843.
(13) Caudle, M. T.; Stevens, R. D.; Crumbliss, A. L. *Inorg. Chem.* **1994**, *33*, 6111.
(14) Caudle, M. T.; Cogswell, L. P., III; Crumbliss, A. L. *Inorg. Chem.* **1994**, *33*, 4759.
(15) Boukhalfa, H.; Crumbliss, A. L. *Inorg. Chem.* **2000**, *39*, 3418.
(16) Boukhalfa, H.; Brickman, T. J.; Armstrong, S. K.; Crumbliss, A. L. *Inorg. Chem.*, Web publication, November 22, 2000.
(17) Colton, R.; D'Agostino, A.; Traeger, J. C. *Mass Spectrom. Rev.* **1995**, *14*, 79.
(18) Gatlin, C. L.; Turecek, F. In *Electrospray Mass Spectrometry; Techniques and Applications*; Cole, R. B., Ed.; Wiley: New York, 1997.
(19) Smith, W. L.; Raymond, K. N. *J. Am. Chem. Soc.* **1980**, *102*, 1252.
(20) Das, M. K.; Roy, N. *J. Chem. Eng. Data* **1984**, *29*, 345.
(21) Spasojević, I.; Armstrong, S. K.; Brickman, T. J.; Crumbliss, A. L. *Inorg. Chem.* **1999**, *38*, 449.

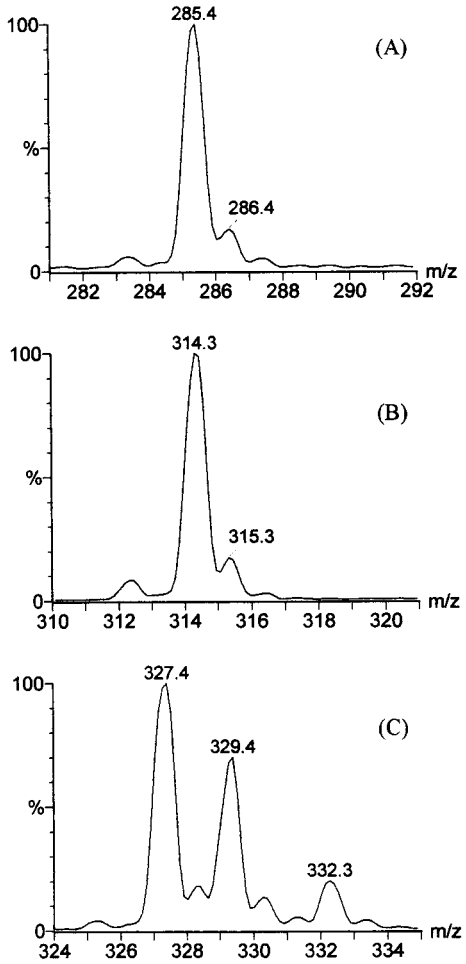

Figure 2. ESI-MS peaks of (A) Al(III)−(H_2L^8), (B) Fe(III)−(H_2L^8), and (C) Ga(III)−(H_2L^8) complexes for M^{3+}/L^8 = 2:3 (M^{3+} = Al^{3+}, Fe^{3+}, and Ga^{3+}), pH 2.3.

redox potentials, the Fe(III)−hydroxamate complexes are stable and those of Fe(II) are likely to be oxidized or undergo decomposition. However, the possible presence of iron(II)−hydroxamate complexes was considered by investigating the corresponding Al(III) and Ga(III) complexes. Al(III) and Ga(III) have similar coordination chemistry characteristics to Fe(III) but do not undergo redox reactions because of the inaccessibility of the +2 oxidation state in aqueous solution. Furthermore, Ga(III) has the advantage of two high natural abundance isotopes that are of particular utility in establishing differences in complex structure, thereby permitting a clear distinction to be made between mono- and bimetallic structures.

Development of Internal Calibrants. The concept of Fe(III) metal replacement by Al(III) or Ga(III) to take advantage of similar charge and metal−ligand affinity, but different isotope distribution, was used to help establish Fe(III)−hydroxamate complex structure and stoichiometry. When Fe^{3+} and a dihydroxamic acid are mixed in a 1:1 ratio, both monometallic ($Fe(L)^+$) and bimetallic ($Fe(L)_2Fe^{2+}$) complexes can be readily formed that are indistinguishable by their UV−visible spectra because both structures possess tetracoordinated iron(III). The ESI-MS spectra of Fe(III), Al(III), and Ga(III) complexes of H_2L^8 prepared in 1:1 M:L ratio at pH 2.3 are shown in Figure 2. The spectrum of the Al(III) complex (Figure 2A) shows a major peak at m/z = 285, which can be due to either $\mathbf{Al(L^8)}^+$ or $\mathbf{Al(L^8)_2Al}^{2+}$. However, the spectrum of the corresponding Fe(III) complex (Figure 2B) shows a major peak at m/z = 314, with satellite peaks at m/z = 312 and 315 corresponding to the

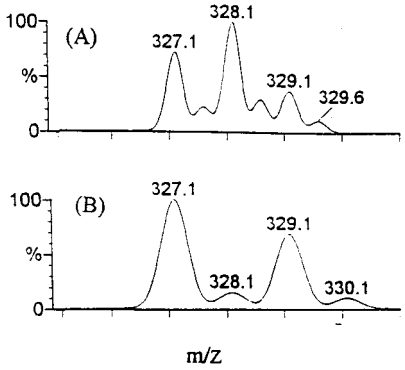

Figure 3. Simulated ESI-MS spectra of Ga(III) complex with H_2L^8: (A) $Ga(L^8)_2Ga^{2+}$, molecular formula $Ga_2(C_{12}H_{22}O_4N_2)_2^{2+}$, and (B) $Ga(L^8)^+$, molecular formula $Ga(C_{12}H_{22}O_4N_2)^+$.

isotopes ^{54}Fe and ^{57}Fe, respectively. Observing the peak related to the ^{54}Fe isotope two units lower than the main peak is a strong argument for assigning these peaks to the monometallic complex $\mathbf{Fe(L^8)}^+$ rather than to the bimetallic complex because $\mathbf{Fe(L^8)_2Fe}^{2+}$ is expected to display a peak at one unit below the main peak at m/z = 313, representing the complex $\mathbf{^{54}Fe(L^8)_2{}^{56}Fe}^{2+}$. This result is confirmed by examining the Ga(III) complex (Figure 2C) where the two isotopes ^{69}Ga and ^{71}Ga are both of high abundance and the difference in the isotopic pattern between the monometallic and the bimetallic complexes is much more easily assigned, as shown in Figure 3.

In contrast to the positively charged monocomplexes, most of the fully coordinated Fe(III) complexes investigated are neutral species, and in an ESI-MS experiment their detection is dependent on ion-clustering. Preliminary spectra of solutions with various electrolytes contained a large number of peaks originating from Na^+, K^+, and Cl^- clusters of the parent molecules. By limiting the electrolyte in the solution to $NH_4{}^+ClO_4{}^-$, we were able to obtain very simple (adduct-peak-free) spectra with high intensities of *intrinsically uncharged* species. Specifically, $NH_4{}^+$ acts as a good proton donor for proton-clustering, which makes neutral molecules detectable and their spectra easier to interpret (only one unit higher in m/z value than the molecular ion peak), while $ClO_4{}^-$ is a noncoordinating anion that does not readily produce adducts with the species of interest. On the other hand, the detection of intrinsically charged species is not dependent on proton-clustering, which makes them more easily detected than intrinsically neutral species. To investigate the difference in detection limits of intrinsically charged vs intrinsically uncharged complexes, we used a mixture of tris-chelated Fe(III) complexes of trihydroxamic acids with +1 (ferrioxamine B^+) and 0 (ferrioxamine E^0) charge as internal standards. Both complexes are very stable and of similar structure, yet one is intrinsically charged (ferrioxamine B^+) and the other is not (ferrioxamine E^0).[2]

Figure 4A shows the ESI-MS spectra for an iron(III)−hydroxamate complex prepared at Fe/L^8 = 2:3, pH 7. The complex was prepared by the addition of 0.5 equiv of H_2L^8 to the Fe/L^8 = 1:1 pH 2 solution followed by neutralization to pH 7 by the addition of 0.1 M NH_4OH. A mixture of **ferrioxamine E^0** (intrinsically neutral at pH 7) and **ferrioxamine B^+** (intrinsically +1 charged at pH 7) was added to this solution in a 9:1 (E^0/B^+) molar ratio as an internal standard. The ESI-MS spectrum for this solution displays a ferrioxamine E^0 peak at m/z = 654 and ferrioxamine B^+ peak at m/z = 614, with a signal intensity ratio of ~6/1, respectively (Figure 4A, Table 2). This somewhat surprising result suggests that under these conditions

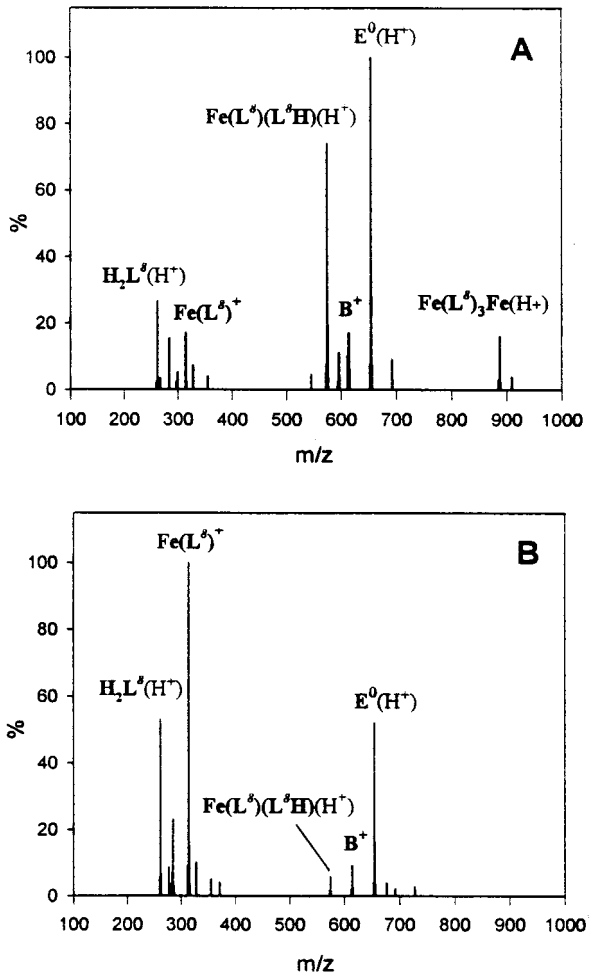

Figure 4. ESI-MS spectrum of Fe(III)−(H_2L^8) system at (A) Fe/L^8 = 2:3, pH 7 and (B) Fe/L^8 = 2:3, pH 2. Conditions are as in Table 2. B^+ and E^0 represent ferrioxamine B and ferrioxamine E, respectively.

intrinsically charged species will appear with (only!) ca. 50% higher intensity than if they were uncharged (with one clustered H^+). The data also show that ferrioxamine B and ferrioxamine E are detected as fully coordinated iron(III) complexes, since in the case of partial protonation of the ligand the peak of the doubly charged ferrioxamine B complex would appear in the spectrum at *m*/*z* = 307.5; however, this is not the case.

At pH 7 and an Fe/L^8 ratio of 2:3 we expect tris-hydroxamate coordination of Fe(III). The ESI spectra of this solution shown in Figure 4A have an intense peak for the $Fe(L^8)^+$ complex, in addition to that for a tris complex $Fe_2(L^8)_3$. This observation indicates a pH drop resulting from solvent evaporation and ionization, resulting in Fe_2L_3 complex dissociation. On the basis of extensive kinetic investigations of the pH-induced dissociation kinetics of ferrioxamine B[26,27] and synthetic linear dihydroxamates,[14,15] we know that the synthetic iron(III)−hydroxamate complexes undergo decomposition to the bis complex at pH = 3. However, ferrioxamine B and ferrioxamine E are much more stable and their dissociation to a bis complex occurs at a much lower pH (pH <2). These data demonstrate that the pair of complexes ferrioxamine B/ferrioxamine E can be used as an internal standard to quantify intrinsically charged and intrinsically neutral iron(III)−hydroxamate complexes.

Data describing the ESI-MS investigation of iron(III) complexes with the synthetic ligands H_2L^2 (Table 1) and H_2L^8 (Table 2), and the natural siderophores rhodotorulic acid (Table 3) and alcaligin (Table 4), will be presented individually in the following sections.

Complexes with the Short-Chain Dihydroxamic Acid $[CH_3N(OH)C(O)]_2(CH_2)_2$ (H_2L^2).[1] The short-chain dihydroxamic acid−Fe(III) system was investigated as a function of pH and Fe/L^2 ratio. At pH 2 and Fe/L^2 = 1:1, the tetracoordinate Fe(III)−dihydroxamate complex is a stable species.[14] On the basis of the isotope pattern of the ESI-MS spectra, it was found previously[13] and in this work that in an aqueous solution the complex exists as a di-Fe, doubly bridged, doubly charged, bis−bis species, $\mathbf{Fe(L^2)_2Fe^{2+}}$, at *m*/*z* 230 [100%]. The existence of this species was confirmed recently by X-ray crystallography.[22] These results are presented in Table 1. The results of subsequent experiments at decreasing Fe/L^2 ratios and increasing pH are also presented in Table 1 and are based on mass spectra such as those presented in Supporting Information (Figure S1). Descriptions of these results at variable Fe/L^2 and pH are presented in the following paragraphs.

Subsequent introduction of an additional equivalent of the ligand (Fe/L^2 = 2:3) and neutralization of the solution to pH 7 results in the formation of a di-Fe tris−tris complex $\mathbf{Fe(L^2)_3Fe^0}$, which in the ESI-MS spectrum appears as $\mathbf{Fe(L^2)_3Fe}(H^+)$ (*m*/*z* 635 [32%]) and $\mathbf{Fe(L^2)_3Fe}(2H^+)$ (*m*/*z* 318 [100%]) (Table 1). The complex is tentatively assigned a triply bridged structure based on two facts: (1) molecular mechanics calculations[13] show that steric strain in the two-carbon chain linking the two hydroxamate groups prevents bis coordination to a single Fe^{3+} center and (2) identification of a doubly bridged structure for $Fe(L^2)_2Fe^{2+}$ was made by X-ray crystallography,[22] which is a precursor to the formation of $Fe(L^2)_3Fe^0$. The peaks at *m*/*z* 635 and 318 may also originate from bis−tris intermediates $\mathbf{(HL^2)Fe(L^2)_2Fe^+}$ and $\mathbf{(HL^2)Fe(L^2)_2Fe^+}(H^+)$, respectively, which in solution may be in a fast bis-to-tris equilibrium with $\mathbf{Fe(L)_3Fe}(H^+)$ and $\mathbf{Fe(L)_3Fe}(2H^+)$.[14] A peak at *m*/*z* 406 [30%] is cautiously ascribed to a di-Fe doubly bridged tris−tris Fe_2L_4 complex $\mathbf{(HL^2)Fe(L^2)_2Fe(L^2H)}(2H^+)$, since it could also be $\mathbf{Fe(L^2H)_2}^+$. The former complex is more likely to occur under our conditions (neutral pH and Fe/L^2 = 2:3), although its one-proton counterpart cluster, $\mathbf{(HL^2)Fe(L^2)_2Fe(L^2H)}(H^+)$, is missing at *m*/*z* 811 (but appears when excess ligand is added; see below). The isotopic pattern for *m*/*z* 406 could not be satisfactorily resolved because of an overlapping unassigned peak at *m*/*z* 407. A strong peak at *m*/*z* 547 [36%] is unambiguously assigned to a bis−tris−tris−bis complex $\mathbf{Fe(L^2)_2Fe(L^2)Fe(L^2)_2Fe^{2+}}$ ($Fe_4L_5^{2+}$) because it is likely a product of the two available species in solution; i.e., $\mathbf{Fe(L^2)_2Fe^{2+}}$ (*m*/*z* 230 [79%]) and $\mathbf{H_2L^2}$ (added at this stage).

Subsequent addition of another equivalent of ligand (Fe/L^2 = 2:4, pH 7) diminishes $\mathbf{Fe(L^2)_2Fe^{2+}}$ (*m*/*z* 230) to 22% and $\mathbf{Fe(L^2)_2Fe(L^2)Fe(L^2)_2Fe^{2+}}$ (*m*/*z* 547) to 25%. At *m*/*z* 318 [100%], $\mathbf{Fe(L^2)_3Fe}(2H^+)$ still dominates the spectrum with its one-proton counterpart $\mathbf{Fe(L^2)_3Fe}(H^+)$ at *m*/*z* 635 [12%]. A new peak at *m*/*z* 811 [10%] is just beginning to appear (see below), and the peak at *m*/*z* 406 is still present with 28% relative intensity. An additional unassigned peak at *m*/*z* 407 occurs in

(22) Boukhalfa, H.; White, P.; Crumbliss, A. L. Manuscript in preparation.
(23) Adventitious potassium adducts are often observed when the mass spectrometer has been previously used to analyze potassium-containing samples, owing to the ubiquitous nature of this element.
(24) Chem 3D software package by Cambridge Soft Corp. (N. L. Allinger's MM2 force field with new terms by J. W. Ponder).
(25) Caudle, M. T.; Caldwell, C. D.; Crumbliss, A. L. *Inorg. Chim. Acta* **1995**, *240*, 519.
(26) Monzyk, B.; Crumbliss, A. L. *J. Am. Chem. Soc.* **1982**, *104*, 4921.
(27) Biruš, M.; Bradić, Z.; Kujundžić, N.; Pribanić, M.; Wilkins, R. G. *Inorg. Chem.* **1985**, *24*, 3980.

Table 1. ESI-MS Data for Fe(III) Complexes with Short-Chain Dihydroxamic Acid $[CH_3N(OH)C{=}O)]_2(CH_2)_2$ (H_2L^2)[a]

			Fe/L^2, pH									
			1:1, pH 2		2:3, pH 7		2:4, pH 7		2:8, pH 7		2:20, pH 7	
species	structure[b]	*m/z* (calcd)	*m/z* (obsd)	%	*m/z* (obsd)	%	*m/z* (obsd)	%	*m/z* (obsd)	%	*m/z* (obsd)	%
$\mathbf{Fe_2(L^2)_2}^{2+}$	$\mathbf{Fe(L^2)_2Fe}^{2+}$	230.0	230.2	100	230.1	79	231.0	22	231.3	25		
$\mathbf{Fe_4(L^2)_5}^{2+}$	$\mathbf{Fe(L^2)_2Fe(L^2)Fe(L^2)_2Fe}^{2+}$	547.1			547.3	36	547.1	25	547.2	12		
$\mathbf{Fe_2(L^2)_3}^0$	$\mathbf{Fe(L^2)_3Fe}(H^+)$	635.2			635.1	32	635.0	12	634.9	33	635	25
$\mathbf{Fe_2(L^2)_3}^0$	$\mathbf{Fe(L^2)_3Fe}(2H^+)$	318.1			318.3	100	318.3	100	318.3	100	318.3	28
$\mathbf{Fe_2(L^2)_2(L^2H)_2}^0$	$\mathbf{(HL^2)Fe(L^2)_2Fe(L^2H)}(H^+)$	811.3					811.1	10	811.1	68	811.1	72
$\mathbf{Fe_2(L^2)_2(L^2H)_2}^0$	$\mathbf{(HL^2)Fe(L^2)_2Fe(L^2H)}(2H^+)$	406.2			406.2	30	406.2	28	406.2	30	406.2	28
$\mathbf{Fe(L^2H)_3}^0$	$\mathbf{Fe(L^2H)_3}(H^+)$	582.4			582.0	4	582.0	4	582.0	35	582.0	100
$\mathbf{(L^2H_2)_2}$	$\mathbf{(H_2L^2)(L^2H_2)}(H^+)$	353.4							353.2	25	353.2	88

[a] Conditions: $[Fe]_{tot}$ = 1 mM; $[H_2L^2]$ = 1−10 mM; $[NH_4^+]$ = 3 mM at pH 2, 14 mM at pH 7; $[ClO_4^-]$ = 14 mM; cone voltage = 40 V. All percentages given are relative to the peak of highest (100%) intensity among Fe-containing species in a particular column (ESI-MS spectrum). See Figure S1 of Supporting Information for mass spectra corresponding to data in Table 1. [b] See ref 1.

Table 2. ESI-MS Data for Fe(III) Complexes with Long-Chain Dihydroxamic Acid $[CH_3N(OH)C{=}O)]_2(CH_2)_8$ (H_2L^8) and Ferrioxamines B and E[a]

			Fe/L^8, pH													
			1:1, pH 2[a]		2:3, pH 7[b]				2:3, pH 2[c]		2:4, pH 7[b]				2:20, pH 7[a]	
species	structure[d]	*m/z* (calcd)	*m/z* (obsd)	%[e]	*m/z* (obsd)	%[e] ESI	*m/z* (obsd)	%[e] FAB	*m/z* (obsd)	%[e]	*m/z* (obsd)	%[e] ESI	*m/z* (obsd)	%[e] FAB	*m/z* (obsd)	%[e]
$\mathbf{L^8H_2}$	$\mathbf{HL^8H}(H^+)$	261.3			261.3	26			261.3	102	261.7	>100	261.2	100	261.2	>100
$\mathbf{Fe(L^8)}^+$	$\mathbf{(L^8)Fe}^+$	314.2	314.4	100	314.4	17			314.5	190[f]	314.4	6	314.4	4		
$\mathbf{Fe_2(L^8)_3}^0$	$\mathbf{Fe(L^8)_3Fe}(H^+)$ $\mathbf{(L^8)Fe(L^8)Fe(L^8)}(H^+)$	887.7			887.5	15	887.3	12			887.4	8	887.1	6		
$\mathbf{Fe(L^8)_2H}^0$	$\mathbf{(L^8)Fe(L^8H)}(H^+)$	574.5			574.6	74	574.2	100	574.6	6	574.6	97	574.2	100	574.2	100
$\mathbf{(L^8H_2)_2}$	$\mathbf{(H_2L^8)(L^8H_2)}(H^+)$	521.6													521.6	10
ferrioxamine E	$\mathbf{FedfE}^0$	654.3			654.3	100			654.3	100	654.3	100				
ferrioxamine B$^+$	$\mathbf{FeHdfB}^+$	614.3			614.3	17			614.3	14	614.3	15				

[a] Conditions: $[Fe]_{tot}$ = 1 mM; $[H_2L^8]$ = 1−10 mM; $[NH_4^+]$ = 3 mM at pH 2, 14 mM at pH 7; $[ClO_4^-]$ = 14 mM; cone voltage = 40 V. See Figure S2 of Supporting Information for mass spectra corresponding to data in Table 2. [b] $[E^0]$ = 0.45 mM; $[B^+]$ = 0.05 mM; $[Fe]_{tot}$ = 0.5 mM; $[H_2L^8]$ = 0.75 and 1 mM; $[NH_4^+]$ = 14 mM; $[ClO_4^-]$ = 14 mM. [c] $[E^0]$ = 0.225 mM; $[B^+]$ = 0.025 mM; $[Fe]_{tot}$ = 0.25 mM; $[H_2L^8]$ = 0.375; $[NH_4^+]$ = 14 mM; $[ClO_4^-]$ = 14 mM. [d] See ref 1. [e] All percentages given are relative to the peak of highest (100%) intensity among Fe-containing species in a particular column (ESI-MS spectrum). [f] Percentage relative to the intensity of ferrioxamine E peak.

this spectrum and subsequent spectra along with the peak at *m/z* 811.

Further addition of ligand (Fe/L^2 = 2:8, pH 7) causes the peak at *m/z* 811 to become the second largest peak in the spectrum with a relative intensity of 68% (Table 1). The species that corresponds to this *m/z* value is a doubly bridged tris−tris complex $\mathbf{(HL^2)Fe(L^2)_2Fe(L^2H)}(H^+)$, which is expected to exist at higher ligand concentrations. The two-proton cluster counterpart $\mathbf{(HL^2)Fe(L^2)_2Fe(L^2H)}(2H^+)$ at *m/z* 406 also appears in the spectra. This observation is in accordance with the expectation that the efficiency of the clustering of protons to a metal complex should not depend on ligand concentration and proves that the peaks belong to the same molecule with one or more protons clustered. Another species, tris−bis $\mathbf{(HL^2)_2Fe(L^2)Fe(L^2H)}^+$, could be a candidate for the *m/z* 811 [68%] peak, since its structure is a likely precursor for the observed $\mathbf{Fe(L^2H)_3}(H^+)$ complex at *m/z* 582 [35%]. The largest increase in the $\mathbf{Fe(L^2H)_3}(H^+)$ species (*m/z* 582) in solution comes from changing the Fe/L^2 ratio from 2:8 to 2:20 (35−100%), accompanied by a drop in $\mathbf{Fe(L^2)_3Fe}(2H^+)$ (*m/z* 318) intensity from 100% to 28%. However, at the same time the *m/z* 811 peak remains unaffected by such an increase in ligand concentration. The absence of $\mathbf{(HL^2)_2Fe(L^2)Fe(L^2H)_2}(2H^+)$ at *m/z* 581 as an anticipated product of $\mathbf{(HL^2)_2Fe(L^2)Fe(L^2H)_2}^+$ and excess ligand $\mathbf{L^2H_2}$ further supports the assignment of the *m/z* 811 peak to the doubly bridged tris−tris complex $\mathbf{(HL^2)Fe(L^2)_2Fe(L^2H)}(H^+)$. A ligand dimer $\mathbf{(L^2H_2)_2}(H^+)$ appears at *m/z* 353 with 25% relative intensity. Obviously, despite high solubility in water, a solution containing ∼2 mM H_2L^2 ligand has a rather strong tendency to form a metal-free dimeric species. This species is interesting because it can be viewed as being "preorganized" for the formation of the doubly bridged bis−bis $Fe(L^2)_2Fe^{2+}$ complex.

At high ligand concentration, i.e., Fe/L^2 = 2:20 and pH 7, the peak that is due to $\mathbf{Fe(L^2H)_3}(H^+)$ reaches its maximum intensity (*m/z* 582, 100%). Another large peak belongs to the ligand dimer, i.e., $\mathbf{(L^2H_2)_2}(H^+)$ (*m/z* 353, 88%). The species at *m/z* 635 originating from either triply bridged tris−tris $\mathbf{Fe(L^2)_3Fe}$ or tris−bis $\mathbf{(HL^2)Fe(L^2)_2Fe}^+$ complex is still present with 25% relative abundance, suggesting a very high stability for such species even under conditions of high excess ligand.

Complexes with the Long-Chain Dihydroxamic Acid $[CH_3N(OH)C(O)]_2(CH_2)_8$ (H_2L^8).[1] The long-chain dihydroxamic acid−Fe(III) system was investigated as a function of pH and Fe/L^8 ratio. At pH 2 and Fe/L^8 = 1:1, the tetracoordinate (bis) Fe(III)−dihydroxamate complex is a stable species.[14] On the basis of isotope patterns observed in ESI-MS spectra, it was established previously[13] and confirmed in this work that in an aqueous solution the 1:1 complex exists as a mono-Fe, singly charged bis species $\mathbf{Fe(L^8)}^+$ at *m/z* 314 [100%]. These results are presented in Table 2. The results of subsequent experiments at decreasing Fe/L^8 ratios and increasing pH are also presented in Table 2 and are based on mass spectra such as are presented in Supporting Information (Figure S2). A description of these results at variable Fe/L^8 and pH is presented in the following paragraphs.

At pH 7 and Fe/L^8 = 2:3 the relative intensity of the bis $\mathbf{Fe(L^8)}^+$ (*m/z* = 314) is reduced to 17% (relative to a DFE

standard and not corrected for the 1:5 relative sensitivity factor for charged and uncharged ions as described above; see Table 2). The most abundant species in this solution is **(L^8)Fe-(L^8H)**(H^+) at *m/z* 574 [74%]. Supporting evidence for this assignment is as follows. The same *m/z* value (574) would appear for a mono-Fe bis $Fe(HL^8)_2^+$ species, a di-Fe singly bridged tris−bis $(HL^8)_2Fe(L^8)Fe(L^8H)^+(H^+)$ species, and a di-Fe doubly bridged tris-tris $(HL^8)Fe(L^8)_2Fe(L^8H)(2H^+)$ species. However, the isotopic pattern of the *m/z* 574 peak corresponds to a calculated isotopic pattern for a singly charged and mono-Fe species. Furthermore, no peak at *m/z* 1148 corresponding to the di-Fe, singly charged species $(HL^8)_2Fe(L^8)Fe(LH^8)^+$ or $(HL^8)Fe(L^8)_2Fe(L^8H)(H^+)$ was found. Also, the mono-Fe bis species $Fe(L^8H)_2^+$ is not likely to exist at neutral pH and a ligand concentration sufficient for complete Fe coordination, i.e., Fe/L^8 = 2:3, pH 7. Addition of ligand (Fe/L^8 = 2:4 and 2:20; Table 2) would diminish a *m/z* 574 peak if due to $\mathbf{Fe(L^8H)_2}^+$ to produce a $\mathbf{Fe(L^8H)_3}$ complex (*m/z* = 837). This was not observed. Final proof for the presence of **(L^8)Fe(L^8H)** was obtained from measurements of mixed-metal solutions (see below). The tris−tris $Fe_2L_3^0$ complex (**$((L^8)Fe(L^8)Fe(L^8)(H^+)$** or **$Fe(L^8)_3Fe(H^+)$**), which was expected to be the major species at pH 7, Fe/L^8 = 2:3, was found at *m/z* 887 with an unexpectedly low relative intensity of 15%. The two-proton counterpart at *m/z* 444 was detected in only a trace amount.

A pH 2 and Fe/L^8 = 2:3 solution was prepared by mixing an Fe/L^8 = 2:3, pH 7 solution in a 1:1 ratio with 0.02 M $HClO_4$. Five minutes after mixing, the solution was injected into the mass spectrometer and the resulting ESI-MS spectrum is shown in Figure 4B. This drop in pH at Fe/L^8 = 2:3 results in almost complete disappearance of the *m/z* 574 peak and the appearance of major peaks at *m/z* 314 and 261 (Table 2). This is consistent with a H^+-driven ligand dissociation from **(L^8)Fe(L^8H)** (*m/z* = 574 for **$(L^8)Fe(L^8H)(H^+)$** to produce **$Fe(L^8)^+$** (*m/z* = 314) and L^8H_2 (*m/z* = 261 for $L^8H_2(H^+)$. This tris-to-bis complex dissociation by protonation to produce a stable **$Fe(L^8)^+$** species is the same as observed in a parallel stopped-flow pH jump kinetics study monitored by UV−vis spectral changes.[15] The intensities observed in the ESI-MS spectrum are in full accordance with our UV−vis kinetic data and confirm the above result that an intrinsically charged species (e.g., **$Fe(L^8)^+$**, *m/z* 314 expected to be present as ∼100% of $Fe(III)_{tot}$ = 0.5 mM) will appear in an ESI-MS spectrum with no more than twice the intensity of an intrinsically neutral species (e.g., **ferrioxamine $E^0(H^+)$**, *m/z* 654, present at 0.45 mM). The signal at 14% intensity (expected 20% relative to the ferrioxamine E^0 peak) *m/z* 614 related to the intrinsically charged **ferrioxamine B^+** present in solution at 0.05 mM further demonstrates the validity of the above assumption. This result is also important because it demonstrates the high reliability of a ferrioxamine E^0/B^+ mixture as an internal standard. The ferrioxamine E^0/B^+ mixture can provide a reasonably accurate quantification of intrinsically charged species relative to intrinsically neutral species in an aqueous solution of iron−hydroxamate complexes probed by ESI-MS.

A pH 7, Fe/L^8 = 2:4 solution was produced by adding 1 equiv of H_2L^8 to the Fe/L^8 = 2:3, pH 7 solution. The dominant complex signal is at *m/z* 574 [100%] and is assigned to the tris complex **$(L^8)Fe(L^8H)(H^+)$**. Minor signals associated with **$Fe(L^8)^+$** (*m/z* 314) and **$Fe(L^8)_3Fe(H^+)$** (*m/z* 887) are present along with an intense signal for the free ligand $H_2L^8(H^+)$ at *m/z* 261 (see Table 2).

A large excess of ligand, i.e., M/L^8 ≈ 2:20, pH 7, results in an ESI-MS spectrum that has only a *m/z* 574 [100%] peak for

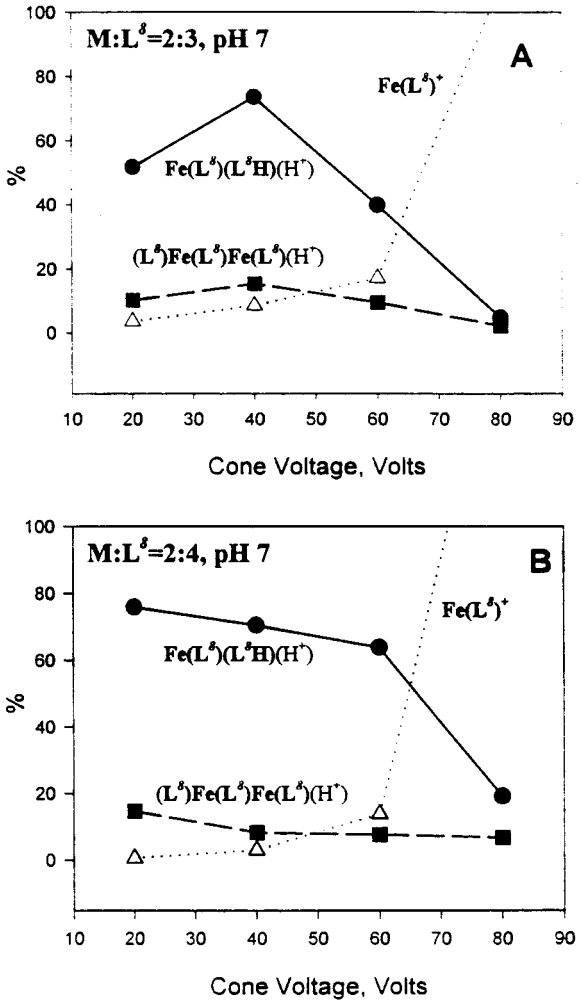

Figure 5. Signal intensity (%) for Fe(L^8)(L^8H), $Fe_2(L^8)_3$ and Fe(L^8)$^+$ plotted as a function of cone voltage at pH 7 and (A) Fe/L^8 = 2:3 and (B) Fe/L^8 = 2:4. Conditions are as in Table 2 except the Fe(L^8)$^+$ signal intensity was corrected (divided) by a factor of 1.5 as described in the text. For reasons of clarity the Fe(L^8)$^+$ intensity at 80 V is out of scale; for the actual values please refer to Table 2.

$(L^8)Fe(L^8H)(H^+)$, a high-intensity peak for the free ligand **$L^8H_2(H^+)$** at *m/z* 261 [≫100%], and a peak for the ligand dimer **$(L^8H_2)_2(H^+)$** at 521 [10%] (Table 2). It is noteworthy that the H_2L^8 ligand is obviously much less prone to dimerization than its short-chain analogue H_2L^2. Also, contrary to the case for the H_2L^2 ligand, the Fe(L^8H)$_3$ complex was not observed, even at very high ligand concentrations (Tables 1 and 2; Fe/L = 2:20). No trace of (L^8)Fe(L^8)Fe(L^8)(H^+) at *m/z* 887.7 or of Fe(L^8)$^+$ at *m/z* 314.2 was found under these conditions.

Fe−Ga and Fe−Al Mixed-Metal Complexes of H_2L^8. 1. Complexes at Low pH. The ESI-MS spectra of a solution with stoichiometry Fe/Al/L^8 = 0.5:0.5:1 at pH 2.3 contain strong peaks at *m/z* = 285, 314, 698, and 727 (40%, 100%, 5%, and 10% respectively) (Figure S4 of Supporting Information). Adduct peaks at *m/z* 427 (16%) and 398 (8%) were also observed and attributed to the parent peaks at 285 and 314, respectively. The spectra of a solution containing Fe/Ga/L^8 = 0.5:0.5:1 at pH 2.3 show strong peaks at *m/z* = 314, 327, 727, and 740 (100%, 42%, 10%, and 5%, respectively) (Figure S5 of Supporting Information). Interpretation of the isotopic pattern for the peak at *m/z* 314 in the two spectra is consistent with the peak being attributed to the mono-Fe complex **$Fe(L^8)^+$**. The weak satellite peak at *m/z* 312 in Figures S4 and S5 corresponds to the ^{54}Fe isotope (natural abundance 2.2%) forming **$^{54}Fe(L^8)^+$**.

Table 3. ESI-MS Data for Fe(III) Complexes with Rhodotorulic Acid (H_2L^{RA})[a]

			Fe/L^{RA}, pH									
			1:1, pH 2		1:1, pH 7		2:3, pH 7		2:4, pH 7		2:20, pH 7	
species	structure[b]	*m/z* (calcd)	*m/z* (obsd)	%	*m/z* (obsd)	%	*m/z* (obsd)	%	*m/z* (obsd)	%	*m/z* (obsd)	%
$\mathbf{H_2L^{RA}}$	$\mathbf{HL^{RA}H}(H^+)$	345.4		0			345.6	35	345.6	>100	345.8	>100
$\mathbf{Fe(L^{RA})^+}$	$\mathbf{(L^{RA})Fe^+}$	398.2	398.4	100	398.3	100	398.2	100	398.5	80	398.3	40
$\mathbf{Fe_2(L^{RA})_3^0}$	$\mathbf{Fe(L^{RA})_3Fe}(2H^+)$	570.4					570.2	10	570.3	10		
	$\mathbf{(L^{RA})Fe(L^{RA})Fe(L^{RA})}(2H^+)$											
$\mathbf{Fe(L^{RA})_2H^0}$	$\mathbf{(L^{RA})Fe(L^{RA}H)}(H^+)$	742.6			742.3	10	742.4	25	742.6	100	742.6	100

[a] Conditions: $[Fe]_{tot} = 1$ mM; $[H_2L^{RA}] = 1-10$ mM; $[NH_4^+] = 3$ mM at pH 2, 14 mM at pH 7; $[ClO_4^-] = 14$ mM; cone voltage = 40 V. All percentages given are relative to the peak of highest (100%) intensity among Fe-containing species in a particular column (ESI-MS spectrum). See Figure S3 of Supporting Information for mass spectra corresponding to data in Table 3. [b] See ref 1.

Table 4. ESI-MS Data for Fe(III) Complexes with Alcaligin (H_2L^{AG})[a]

			Fe/L^{AG}, pH											
			1:1, pH 2		1:1, pH 7		2:3, pH 7		2:4, pH 7		2:8, pH 7		2:8, pH 9.5	
species	structure[b]	*m/z* (calcd)	*m/z* (obsd)	%	*m/z* (obsd)	%	*m/z* (obsd)	%	*m/z* (obsd)	%	*m/z* (obsd)	%	*m/z* (obsd)	%
$\mathbf{H_2L^{AG}}$	$\mathbf{HL^{AG}H}(H^+)$	405.4		0			405.5	80	405.4	>100	405.5	>100	405.5	>100
$\mathbf{Fe(L^{AG})^+}$	$\mathbf{(L^{AG})Fe^+}$	458.3	458.3	100	458.4	100	458.4	100	458.4	73				
$\mathbf{Fe_2(L^{AG})_3^0}$	$\mathbf{Fe(L^{AG})_3Fe}(H^+)$	1319.9					1320.7	10[c]						
	$\mathbf{(L^{AG})Fe(L^{AG})Fe(L^{AG})}(H^+)$													
$\mathbf{Fe_2(L^{AG})_3^0}$	$\mathbf{Fe(L^{AG})_3Fe}(2H^+)$	660.5					660.6	40	660.3	53	660.3	10	660.3	4
	$\mathbf{(L^{AG})Fe(L^{AG})Fe(L^{AG})}(2H^+)$													
$\mathbf{Fe(L^{AG})_2H^0}$	$\mathbf{(L^{AG})Fe(L^{AG}H)}(H^+)$	862.7			862.4	5	862.6	10	862.1	100	862.2	100	862.2	100

[a] Conditions: $[Fe]_{tot} = 1$ mM; $[H_2L^{AG}] = 1-4$ mM; $[NH_4^+] = 3$ mM at pH 2, 14 mM at pH 7; $[ClO_4^-] = 14$ mM; cone voltage = 40 V. All percentages given are relative to the peak of highest (100%) intensity among Fe-containing species in a particular column (ESI-MS spectrum).[b] See ref 1. [c] Cone voltage = 70 V.

The doubly charged complex $Fe(L^8)_2Fe^{2+}$ is also expected to display a peak at $m/z = 314$. However, the double charge on the molecule would "compress" the isotopic pattern, and the peak corresponding to $^{54}Fe(L^8)_2{}^{56}Fe^{2+}$ would in such a case appear at only one *m/z* unit lower (*m/z* 313) than the peak of the parent $^{56}Fe(L^8)_2{}^{56}Fe^{2+}$ molecule (*m/z* 314).[12,13] Thus, the presence of a satellite peak at *m/z* 312 is in agreement with assignment of the peak at *m/z* 314 to the monometallic complex $\mathbf{^{56}Fe(L^8)^+}$. The spectra of the Ga-containing complexes, where the ^{69}Ga isotope is naturally abundant at 60.2% and ^{71}Ga at 39.8%, show a greater isotopic pattern difference between mono- and bimetallic complexes than the corresponding Fe complexes (^{56}Fe, ^{54}Fe, and ^{57}Fe natural abundances are 91.52, 5.90, and 2.25%, respectively). This makes the assignment of peaks more unambiguous as illustrated in Figure 3. The peak at $m/z = 327$, when compared to the simulated isotopic peak pattern, confirms the monometallic structure $\mathbf{Ga(L^8)^+}$ for the observed species. The peak at *m/z* 285 in the Fe−Al solution (Figure S4 of Supporting Information) is attributed to the $\mathbf{Al(L^8)^+}$ complex by analogy with the Fe and Ga complexes. The peaks at *m/z* 727 and 740 in the spectra of the Fe−Ga solution are attributed to $\mathbf{Fe(L^8)_2Fe}(ClO_4)^+$ and $\mathbf{Fe(L^8)_2Ga}(ClO_4)^+$, respectively, by comparison between the experimental and simulated spectra. The spectra obtained for the Fe−Al solution display peaks at *m/z* 727 and 698 and are attributed to the complexes $\mathbf{Fe(L^8)_2Fe}(ClO_4)^+$ and $\mathbf{Fe(L^8)_2Al}(ClO_4)^+$. The $\mathbf{M(L^8)_2M}(ClO_4)^+$ complexes adopt a bimetallic doubly bridged structure. These results clearly demonstrate that the bis Fe complex of H_2L^8 is present in aqueous solution as a mixture of mono- and di-Fe species rather than only mono-Fe species, as was interpreted from our previous work.[13]

2. Complexes at Neutral pH. The ESI-MS spectra of solutions with a stoichiometry Ga/Fe/L^8 = 1:1:3 at pH 7 show peaks at *m/z* 314, 327, 574, 587, 887, and 900 (100%, 37%, 32%, 15%, 10%, and 7% respectively) (Figure S6 of Supporting Information). Other peaks at 427 (45%), 442 (18%), 900 (5%), and 938 (5%) are also observed. However, peaks at 427 and 442 are adducts of the parent peaks at *m/z* 314 and 327 (131 mass unit cluster), and the peaks at 612 and 625 are the result of potassium clustering to the parent peaks at 574 and 587.[21] The peak at *m/z* 574 represents a monometallic Fe species and can be attributed either to $\mathbf{(L^8)Fe(L^8H)}(H)^+$ or to $\mathbf{Fe(L^8H)_2}^+$. The corresponding Ga-containing species, $\mathbf{(L^8)Ga(L^8H)}(H)^+$ or $\mathbf{Ga(L^8H)_2}^+$, appears at *m/z* 587. Examination of the isotopic pattern cannot distinguish between these two species. However, the presence of the adducts at 612 and 625 due to clustering of the potassium to the parent peak at 574 and 587 is in good agreement with the assignment of the parent peaks to the originally neutral complexes $\mathbf{(L^8)Fe(L^8H)}(H^+)$ and $\mathbf{(L^8)Ga(L^8H)}(H^+)$ rather than to $\mathbf{Fe(L^8H)_2}^+$ and $\mathbf{Ga(L^8H)_2}^+$, where the positive charge on the complex $\mathbf{M(L^8H)_2}^+$ should prevent the potassium from forming a doubly charged species $\mathbf{M(L^8H)_2}^+(K^+)$. The absence of peaks at *m/z* 306 and 312 representing the clusters $\mathbf{Fe(L^8H)_2}^+(K^+)$ and $\mathbf{Ga(L^8H)_2}^+(K^+)$ is additional support for assigning the parent peaks to $\mathbf{(L^8)Fe(L^8H)}(H^+)$ and $\mathbf{(L^8)Ga(L^8H)}(H^+)$ rather than to $Fe(L^8H)_2^+$ and $Ga(L^8H)_2^+$, respectively.

Cone Voltage. To address the possibility that an FeL_2H^0 complex could be generated from $Fe_2L_3^0$ in the course of the ESI-MS experiment (and not initially present in solution), an experiment varying the *cone voltage* was conducted using Fe/L^8 = 2:3, pH 7 (Figure 5A) and Fe/L^8 = 2:4, pH 7 (Figure 5B) solutions containing ferrioxamine E^0/B^+ as an internal standard. The plots in Figure 5 clearly demonstrate that for a wide range of cone voltages (20−60 V), the ratio of $\mathbf{(L^8)Fe(L^8H)}(H^+)$ to $\mathbf{Fe(L^8)_3Fe}(H^+)$ remains unchanged. It is only at a very high cone voltage (80 V) that the $(L^8)Fe(L^8H)^0$ complex is collisionally dissociated to give a large amount of intrinsically charged $Fe(L^8)^+$ species.

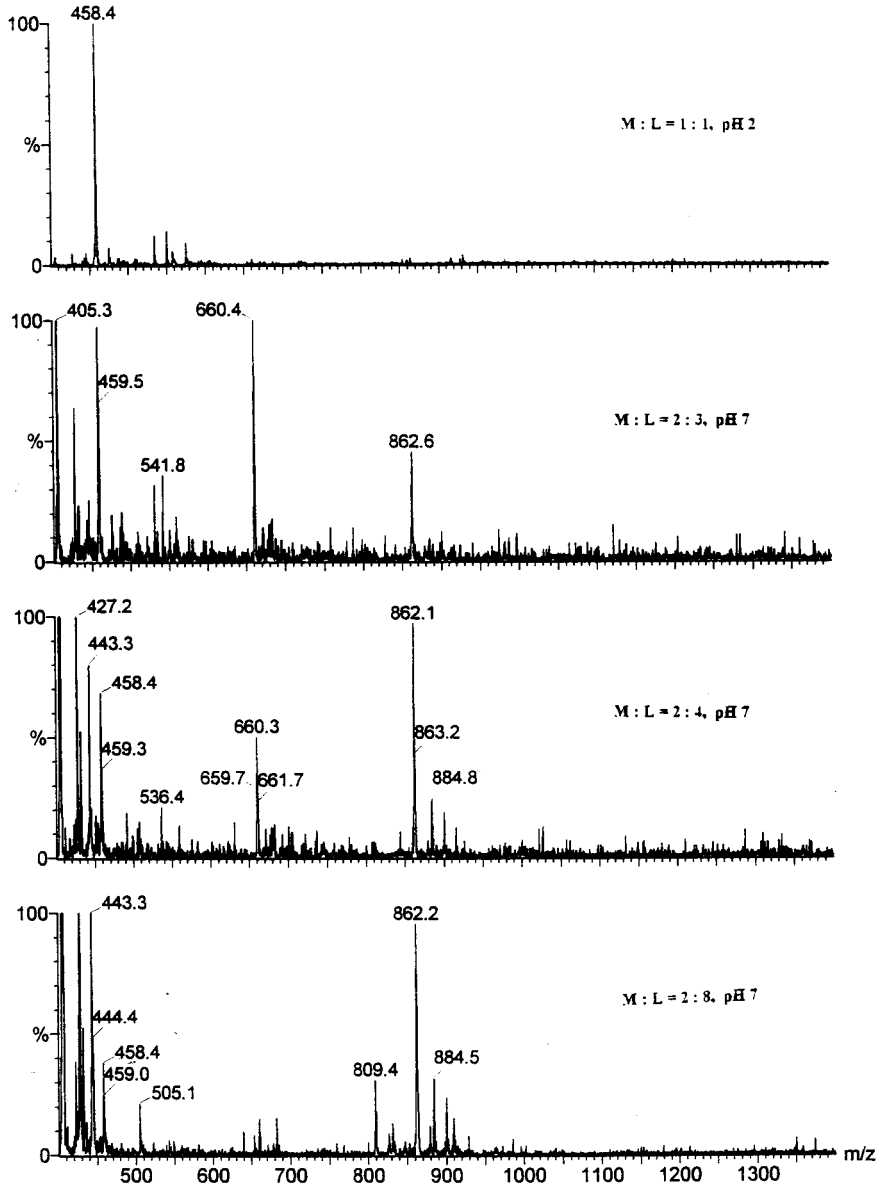

Figure 6. ESI-MS spectra of Fe(III)−alcaligin (H_2L^{AG}) system at different Fe/L^{AG} ratios and solution acidities. Conditions and data are as in Table 4.

Fast-Atom-Bombardment (FAB) Mass Spectrometry. FAB-MS was used to confirm our results using ESI-MS because of its different ionization mechanism. Table 2 shows the intensities of Fe(III)−(L^8) species of interest taken from the FAB spectra of Fe/L^8 = 2:3 and Fe/L^8 = 2:4 solutions at pH 7. The results are in full agreement with the conclusions drawn from ESI-MS spectra. Thus, on the basis of identical results obtained using two different ionization techniques, we conclude that although the tris-$Fe_2(L^8)_3^0$ species may be a major species in aqueous solution, it is very labile and in a tris-to-bis proton hydrolysis reaction will lead to the more stable intermediate tris (L^8)Fe-(L^8H)^0. At the other extreme, the results suggest that in an equilibrated solution of Fe(III)−(L^8), even at Fe/L^8 = 2:3 and pH 7, much of the tris complex is in the (L^8)Fe(L^8H)^0 form and only a fraction exists as the $Fe_2(L^8)_3^0$ species.

Rhodotorulic Acid (H_2L^{RA}).[1] Rhodotorulic acid (H_2L^{RA}) is a linear dihydroxamic acid siderophore (Figure 1). ESI-MS spectra, acquired using Fe/L^{RA} = 1:1, pH 2 solutions prepared in the same manner as in the case of the synthetic ligands, very closely resemble the data collected for the long-chain Fe/L^8 system (Table 3). The six-atom ring in the rhodotorulic acid backbone apparently does not significantly influence the flexibility of the otherwise long carbon chain between hydroxamate moieties, since it forms a mono-iron bis-**Fe(L^{RA})**$^+$ species instead of a doubly bridged Fe(L^{RA})$_2$Fe^{2+} structure. The Fe nuclearity was confirmed here and previously[13] by the isotopic pattern assigned to the Fe(L^{RA})$^+$ peak at *m*/*z* 398. ESI-MS spectra (Table 3 and Figure S3 of Supporting Information) for Fe/L^{RA} = 1:1 and Fe/L^{RA} = 2:3 pH 7 solutions show large amounts of **Fe(L^{RA})**$^+$ species presumably because of being easily detectable (intrinsically charged) or being a fragment of Fe(L^{RA})(OH). This peak, however, gradually diminishes with further addition of ligand in solution (Table 3 and Figure S3 of Supporting Information). The peak at *m*/*z* 742 corresponding to the **(L^{RA})Fe($L^{RA}H$)**(H^+) species is present as a major peak for tris-Fe species at all Fe/L^{RA} ratios at pH 7. The uncharged di-Fe species $Fe_2(L^{RA})_3^0$ appears only as a two-proton clustered ion (either the singly bridged **(L^{RA})Fe(L^{RA})Fe(L^{RA})**($2H^+$) or triply bridged **Fe(L^{RA})$_3$Fe**($2H^+$) species at *m*/*z* 570) and reaches its maximum abundance (40% abundance relative to the **(L^{RA})Fe($L^{RA}H$)**(H^+) peak at *m*/*z* 742; 10% abundance relative to the **Fe(L^{RA})**$^+$ peak at *m*/*z* 398; Table 3) at Fe/L^{RA} = 2:3 and

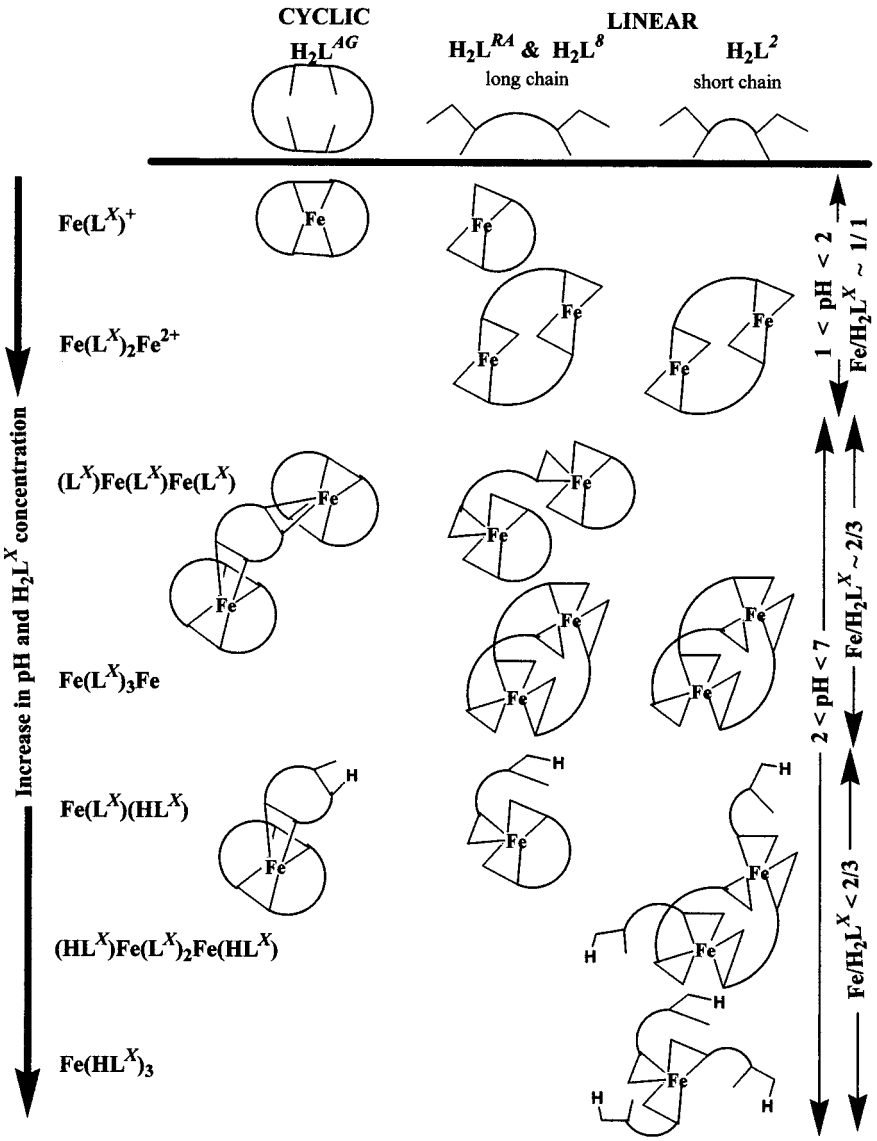

Figure 7. Speciation of Fe(III)−dihydroxamate complexes present in aqueous solution at variable Fe/L ratios and pH as determined by ESI-MS. Certain structures are eliminated from consideration as follows: $Fe(L^{AG})_2Fe^{2+}$ because there is no ESI-MS evidence for this species; $Fe(L^{AG})_3Fe$ is eliminated on the basis of the crystal structure for $Fe_2(L^{AG})_3$, which shows a single ligand bridge structure, $(L^{AG})Fe(L^{AG})Fe(L^{AG})$;[10] $Fe(L^{RA})_2Fe^{2+}$ is eliminated because there is no ESI-MS evidence for this species; $Fe(L^2)^+$ is eliminated because there is no ESI-MS evidence for this species, consistent with molecular mechanics calculations that demonstrate that the $(L^2)^{2-}$ ligand cannot act as a tetradentate ligand to a single Fe(III) center;[13] $(L^2)Fe(L^2)Fe(L^2)$ is eliminated on the basis of molecular mechanics calculations that demonstrate that the $(L^2)^{2-}$ ligand cannot act as a tetradentate ligand to a single Fe(III) center;[13] $Fe(L^2)(L^2H)$ is eliminated because there is no ESI-MS evidence for this species, consistent with molecular mechanics calculations that demonstrate that the $(L^2)^{2-}$ ligand cannot act as a tetradentate ligand to a single Fe(III) center.[13]

pH 7. The further addition of rhodotorulic acid ($Fe/L^{RA} = 2:4$, pH 7) decreases the intensity of the $\mathbf{Fe_2(L^{RA})_3}(2H^+)$ peak, and finally it disappears at very high ligand concentration, i.e., $Fe/L^{RA} = 2:20$, pH 7 (Table 3).

Alcaligin (H_2L^{AG}).[1] Alcaligin (H_2L^{AG}) is a cyclic dihydroxamic acid siderophore (Figure 1). ESI-MS spectra acquired using an $Fe/L^{AG} = 1:1$, pH 2 solution show a simple peak at *m*/*z* 458 with an isotopic pattern consistent with the tetracoordinated $Fe(L^{AG})^+$ (Table 4; Figure 6). This is consistent with the stable preorganized alcaligin structure previously reported.[10,11] At $Fe/L^{AG} = 2:3$, pH 7 the complex $(L^{AG})Fe(L^{AG})Fe(L^{AG})$ previously identified crystallographically[10] appears in both one- and two-proton-clustered forms: $\mathbf{(L^{AG})Fe(L^{AG})Fe(L^{AG})}(H^+)$ at *m*/*z* 1320 [10%] and $\mathbf{(L^{AG})Fe(L^{AG})Fe(L^{AG})}(2H^+)$ at *m*/*z* 660 [40%] as the major tris-Fe species in solution. However, an additional equivalent of ligand, i.e., $Fe/L^{AG} = 2:4$, pH 7, causes the peak for $\mathbf{(L^{AG})Fe(L^{AG}H)}(H^+)$ at *m*/*z* 862 [100%] to prevail among tris-iron species. This result is in accordance with our prediction that the singly bridged $(L^{AG})Fe(L^{AG})Fe(L^{AG})$ species will undergo reaction with excess H_2L^{AG} in solution and form the simpler and entropically preferred $(L^{AG})Fe(L^{AG}H)$ complex. This is also consistent with our kinetic investigation.[16]

Our results in Table 4 illustrate the change in $Fe_2(L^{AG})_3{}^0/Fe(L^{AG})(L^{AG}H)^0$ ratio as the alcaligin concentration increases. In a cone voltage variation experiment (30−70 V), no significant change in the $Fe_2(L^{AG})_3{}^0/Fe(L^{AG})(L^{AG}H)^0$ ratio was observed. Only a change in ratio between one- and two-proton clustered forms of $Fe_2L_3{}^0$ was observed (i.e., $\mathbf{(L^{AG})Fe(L^{AG})Fe(L^{AG})}(H^+)$ and $\mathbf{(L^{AG})Fe(L^{AG})Fe(L^{AG})}(2H^+)$; data not shown), which means that under these conditions only proton loss occurs without decomposition or rearrangement of the Fe−alcaligin complexes.

It should be noted that neither hydroxo- nor μ-oxo-bridged species were observed under these experimental conditions,

despite their observation in a study utilizing potentiometric and spectrophotometric techniques.[11]

Discussion

We have demonstrated that electrospray ionization mass spectrometry (ESI-MS) may be successfully utilized to probe the speciation of both neutral and charged Fe(III)−dihydroxamate siderophore complexes in aqueous solution. By utilizing NH_4^+ as a proton donor and ClO_4^- as a noncoordinating counteranion, we have obtained very simple (adduct peak free) and interpretable spectra for intrinsically neutral Fe(III)−dihydroxamate complexes.

By utilizing different ionization techniques (ESI, FAB), altering the experimental parameters (Fe/L ratio, pH, cone voltage) and using mixed-metal (Fe^{3+}, Al^{3+}, Ga^{3+}) complexes, we were able to obtain important information on the *structure* and the *speciation* of metal−dihydroxamate complexes in aqueous solution. We have also shown that by using an appropriate internal standard (ferrioxamine E^0/ferrioxamine B^+), reasonably accurate quantitative data for solution speciation may be obtained.

Figure 7 summarizes the mono- and dinuclear Fe(III) complexes identified at various Fe/L ratios and solution pH values for the synthetic (H_2L^n) and for rhodotorulic acid (H_2L^{RA}) and alcaligin (H_2L^{AG}) siderophore dihydroxamic acids. When exposed to an excess of alcaligin, rhodotorulic acid, or H_2L^n ligand, in all cases we observe a tendency to form Fe complexes of Fe/L stoichiometry ratio lower than Fe/L = 2:3 (e.g., 1:2 or 1:3; Figure 7). For example, in neutral aqueous solutions with a M/L ratio of 1:2, the short-chain ligand, H_2L^2, forms a di-Fe, doubly bridged tris-$(HL^2)Fe(L^2)_2Fe(L^2H)$ complex, while the other three ligands under the same conditions form the mono-Fe, tris $(L^X)Fe(L^XH)$ ($X = 8$, RA, AG) complex.

Our ESI-MS data also suggest that the di-Fe complex $Fe_2(L)_3$ is a very labile species for all ligands examined. However, despite numerous approaches employed (variation in cone voltage, ligand concentration and pH, use of an internal standard, and complementary ESI/FAB experiments), there is still some ambiguity as to whether (1) the $Fe_2(L)_3$ complex is present in an equilibrated neutral solution but too labile to "survive" the ESI-MS experiment or (2) this species is really unstable and readily forms the simpler (L)Fe(LH) species, even at the expense of leaving some of the Fe(III) coordinatively unsaturated in solution (presumably as FeL(OH),[25] etc.). The short-chain dihydroxamic acid, H_2L^2, differs from the other ligands in its resistance to changing the structure of its Fe_2L_3 complex upon the addition of excess ligand. Also, the short-chain H_2L^2 ligand is unique in its tendency to form an $Fe(L^2H)_3$ complex, which was not found in the case of other ligands, although kinetic data support the transient existence of $Fe(L^8H)_3$.[15]

The fast dissociation of the tris-chelated iron(III) complexes is probably the reason for observing an appreciable amount of the bis complex when analyzing the complex prepared under conditions where the tris complex is more stable (low Fe/L ratio and high pH). The bis-chelated complex structures are more easily characterized relative to the tris-chelated complexes because of their lower lability.[14−16] A pH drop resulting from solvent evaporation in the ESI-MS experiment may result in a partial dissociation of the tris and bis complexes. We have demonstrated from our kinetic investigation that the tris and bis complexes dissociate via multiple paths involving structurally different species,[15,16] which is in good agreement with multiple species observed in the ESI-MS spectra.

Our ESI-MS results demonstrate the presence of multiple mono- and dinuclear Fe(III) species with dihydroxamic acid siderophores and model siderophores that are in dynamic equilibrium. The multiplicity of interconvertible species is a feature that distinguishes Fe(III)−dihydroxamate solutions from their hexadentate trihydroxamate siderophore counterparts. This characteristic may play a role in the use of tetradentate siderophores by organisms for Fe acquisition in that the multiplicity of species may provide for multiple paths for Fe acquisition and release through ligand dissociation/ternary complex formation, molecular recognition, etc.

Acknowledgment. We thank the NSF for financial support and S. K. Armstrong and T. J. Brickman (University of Minnesota) and I. Fridovich (Duke University) for gifts of alcaligin and the ferrioxamines.

Supporting Information Available: Three figures containing experimental spectra corresponding to the data in Tables 1−3 and one figure containing experimental spectra obtained using mixed Fe(III), Ga(III), and Al(III) metals with the long-chain dihydroxamic acid H_2L^8. This material is available free of charge via the Internet at http://pubs.acs.org.

IC991390X